Ball-Tipped Fibers for Laser Angioplasty with the Pulsed-Dye Laser

MARTIN R. PRINCE, GLENN M. LaMURAGLIA, CHRISTINE E. SEIDLITZ, SCOTT A. PRAHL, CHRISTOS A. ATHANASOULIS, AND REGINALD BIRNGRUBER

***Abstract*—A method of introducing high-intensity laser radiation into arteries has been developed and tested in amputated human limbs. The device consists of a small diameter, flexible, quartz optical fiber which tapers to a large diameter, smooth, rounded ball-tip. The smooth, ball-tip minimizes the chance of mechanical dissection or perforation of the vessel wall. The spot size can be varied over a large range by varying the fiber input coupling, taper length, and numerical aperture. With 480 nm radiation, which is preferentially absorbed by atherosclerotic plaque and thrombus, at 8 μs pulse durations, the device effectively recanalized occluded human peripheral arteries creating a 2–3 mm diameter channel. The radiant exposure required to recanalized arteries (85 J/cm^2) was higher than the ablation threshold for plaque (56 J/cm^2), but well below the fluence required to ablate normal artery and perforate (226 J/cm^2). Time-delayed, flash photography demonstrates formation of a large vapor bubble with each ablative pulse which suggests that laser recanalization can involve not only ablating plaque but also an expanding effect similar to balloon angioplasty. These data demonstrate that a tapered ball-tipped fiber can deliver the high-intensity 480 nm radiation required for selective ablation of plaque and this device can effectively recanalize symptomatic peripheral artery occlusions.**

Introduction

LASER angioplasty is a promising method of opening arteries that are obstructed by atherosclerotic plaque. It has potential advantages over surgery, balloon angioplasty, and other forms of vascular interventions. Laser radiation may be introduced into arteries via small optical fibers, thus avoiding major surgery. The radiation can remove plaque rather than displacing it, thus, potentially reducing the high rate of restenosis that occurs with balloon angioplasty. Radiation can be preferentially absorbed by plaque, thereby adding an element of specificity and safety that may not exist with mechanical atherectomy devices.

Manuscript received August 11, 1989; revised January 19, 1990 and September 5, 1990. This work was supported in part by the National Institutes of Health under Fellowship HL07377, by the Arthur O. and Gullan M. Wellman Foundation, by the Stategic Defense Initiative Organization under Contract N00014-86-K-0016, and by the Department of Radiology, Massachusetts General Hospital.

M. R. Prince and C. A. Athanasoulis are with the Department of Radiology and the Wellman Laboratories of Photomedicine, Harvard Medical School, Massachusetts General Hospital, Boston, MA 02114.

G. M. LaMuraglia is with the Department of Vascular Surgery and the Wellman Laboratories of Photomedicine, Harvard Medical School, Massachusetts General Hospital, Boston, MA 02114.

C. E. Seidlitz, S. A. Prahl, and R. Birngruber are with the Wellman Laboratories of Photomedicine, Harvard Medical School, Massachusetts General Hospital, Boston, MA 02114.

IEEE Log Number 9040273.

Early laser angioplasty systems, however, have not taken full advantage of the unique properties of laser radiation. As a result, there have been frequent perforations, dissections, and other problems associated with damage to the underlying normal artery wall [1]–[4]. This inadvertent damage can be categorized as resulting from the laser–tissue interaction or from the laser-delivery system.

Many of the laser–tissue interaction problems are solved by careful selection of laser parameters. The massive thermal injury that occurs with continuous wave lasers can be minimized by using pulse durations that are short enough to make thermal diffusion negligible. This is accomplished with pulse durations that are much shorter than the tissue thermal relaxation time [5]–[8], which is about 100 ms for blue–green radiation from an argon ion laser. Calcified plaque, which could not be removed with low to moderate intensity lasers, is now known to be readily plasma ablated with high-intensity radiation [9]. Specificity for plaque (frequently called selective ablation) is achieved at wavelengths where plaque absorption is much greater than normal artery absorption [10]–[13]. Fine, "precise" ablation is achieved at wavelengths where plaque absorption is strong or can be enhanced with exogenous chromophores [14]–[16].

Laser delivery problems, however, have been more difficult to resolve [17]. The bare, quartz optical fibers that were used initially have been shown to have sharp edges which perforate arteries even when the laser is not on [Fig. 1(a)]. Sanborn *et al.*, with their "hot tip" fiber, have eliminated the sharp end by covering the optical fiber with a rounded, metal cap [18] [Fig. 1(b)]. This rounded, bulbous cap improves the fiber's ability to track arterial lumens and avoid mechanical perforation, but it forgoes the advantages of having laser radiation reach the tissue. Some investigators have melted the end of the optical fiber to form a ball with a similar shape as the "hot tip" [19], [Fig. 1(c)]. This retains the desirable shape but allows all of the laser radiation to reach the tissue; early clinical trials have been encouraging [12]. Unfortunately, for large ball tips, the tip-to-fiber connection tends to be fragile, creating the risk of fracture and embolization.

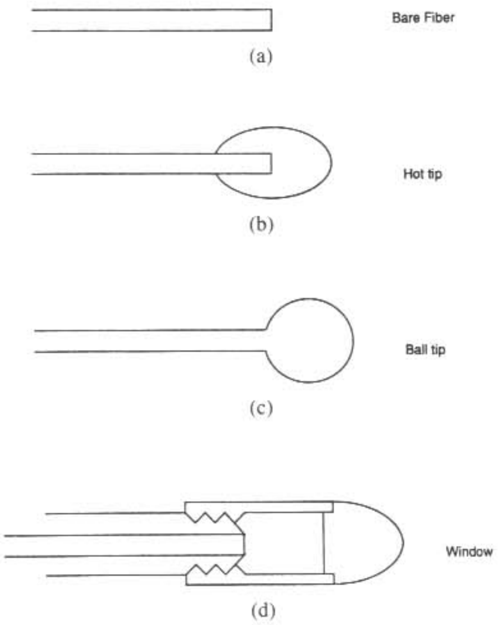

Fig. 1. Optical fiber tips commonly used for laser angioplasty. (a) Bare fibers readily mechanically dissect and perforate arteries due to the sharp edges. (b) The ''hot tip'' is less likely to cause mechanical damage because of its smooth edges, but it does not allow the laser radiation to reach the tissue. (c) Ball tips have smooth edges and allow the light to reach tissue, but the spot size tends to be much smaller than the ball diameter and the fiber is fragile where it was heated near the ball tip, making embolization of the tip possible. (d) A sturdy window design prevents embolization of ball tips and allows some control over the spot size, but it is bulky with a long stiff end.

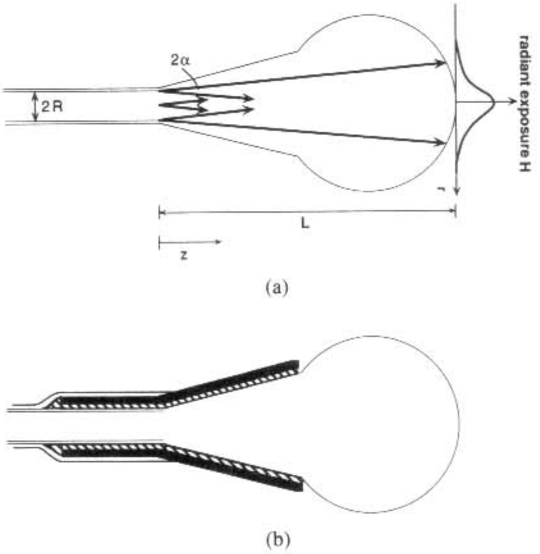

Fig. 2. Schematic of a tapered ball-tip optical fiber. (a) A fiber (top view) with a core diameter $2R$ and taper length $L \gg R$ produces a bell-shaped radiant exposure profile on the tissue surface in contact with the ball tip. (b) The complete device is shown at the bottom with a stainless steel sleeve (thick dark line) glued (hashed area) onto the fiber and a covering layer of heat shrink teflon.

Some of these problems have been overcome by mounting a transparent rounded sapphire or silica window at a fixed distance from the end of the fiber [4], [20]–[22] [Fig. 1(d)]. Using a steel coupler, the window can be firmly attached, thus avoiding the possibility of fracture. The space between the window surface and the fiber tip allows the laser beam to expand. Several problems, however, remain: the dead space may accumulate blood, there is a long stiff end, and the extra interfaces disperse energy increasing the chance of fiber damage and making it difficult to transmit enough high-intensity radiation to effectively ablate calcified plaque.

This paper describes a simple fiber–optic delivery system featuring the advantages of prior designs including a smooth, rounded, atraumatic tip with a variable spot size. There are no optical interfaces within the fiber, it has a short stiff end, good mechanical stability, and is radiopaque. Preliminary testing of this fiber with the pulsed-dye laser in amputated human limbs is also described.

Fiber Design

Flexible, quartz optical fibers with 320, 400, or 600 μm core diameters (Polymicro Technologies, Phoenix, AZ) are melted at the tip to form an end which tapers out to a ball, as shown in Fig. 2(a). The tapered region can, in theory, allow the radiation to expand to a spot size nearly as large as the ball diameter. A stainless steel sleeve makes the tip sufficiently radiopaque to be readily visualized under fluoroscopy. It also provides structural rigidity to the melted region near the ball tip which is weaker than the native fiber. The length of the taper and the stainless steel sleeve determines the length of the ''stiff'' region at the end of the fiber. The stainless steel sleeve and fiber are covered with a thin layer of teflon to eliminate the stainless steel sleeve edge which otherwise would become caught on catheters and sheaths. The teflon also provides a smooth, biocompatible, minimally thrombogenic surface to facilitate manipulations through catheters [Fig. 2(b)].

The teflon-covered 400 μm fiber is similar in diameter and flexibility to the typical 0.035 inch guidewires used in clinical catheterization procedures. By passing catheters coaxially over the fiber it is possible to steer the tip with a curved catheter or to inject fluid near the tip, i.e., saline to displace blood or contrast to visualize the lumen.

Methods of Fabrication

The most difficult part of the device to make is the taper. Heating the fiber end will always form a ball without a taper due to the strong surface tension of molten quartz in air. When fibers are made by drawing from a large diameter boule of quartz, the fiber diameter is determined in part by the rate of pulling on the fiber. Thus, the fiber diameter can be varied by changing the rate of pulling during fiber drawing. This, however, produces an unpredictable taper length and is prohibitively expensive. An alternative, less expensive, and more predictable method is to mount the fiber on a glass lathe and gradually heat a midsection of the fiber with an oxy–methane flame. As the fiber softens and becomes molten, surface tension causes the fiber to slowly shorten and increase in diameter in the molten region. By moving the flame down the fiber, a taper of any shape and length can be formed. Even more precise heating of the fiber can be obtained by using a CO_2 laser instead of a flame. Once the taper is formed, any fiber remaining at the end can be broken off and discarded or melted to form a large ball.

Any melted region of the fiber is flame annealed and then reclad by dipping the fiber into a low-index polyimide cladding material. A stainless steel sleeve with a tapered end is glued on to the tapered region of the fiber with biocompatible epoxy. The final step is covering the fiber–sleeve with heat shrink teflon tubing to protect the fiber and to provide a biocompatible surface.

Light Distribution on the Ball-Tip Surface

Many factors affect the size of the laser radiation spot on the ball surface including the fiber core diameter ($2R$), fiber numerical aperture (NA), taper length (L), and the fiber modes that are excited. A method of calculating the light distribution on the ball surface is given in the Appendix. Equation (2) from the Appendix was integrated numerically to obtain the light distribution for a 7 mm taper on a 400 μm core diameter fiber with the maximum divergence angle

$$\alpha_{\text{maximum}} = \sin^{-1} \frac{\text{NA}}{n_{\text{core}}}$$

as shown in Fig. 3(a) (curve 1). This theoretical maximum divergence, however, is not usually attained because the higher order fiber modes are frequently not excited. In practice, the coupling optics typically used (a 3 mm diameter laser beam with a 50 mm focal length quartz lens) with the standard quartz fiber (numerical aperture = 0.22) produces a divergence angle, $\alpha = 3.4°$, which is much less then $\alpha_{\text{maximum}} = 8.4°$. Thus, the calculated spot size for $\alpha = 3.4°$ is much smaller than the theoretical maximum (see Fig. 3(a), curve 2). This was verified experimentally by measuring the light distribution with a 50 μm fiber detector scanned across the ball-tip surface.

Because this Gaussian distribution is related to which fiber modes are excited, considerable variation in spot size can be achieved by exciting different modes. This can be accomplished by varying the angle of optical coupling into the fiber. Short focal length lenses with a large laser beam diameter can fill both low and high-order fiber modes and create a large spot size while longer focal length lenses will excite primarily low-order modes and create a small spot size. If light is coupled into only lower order fiber modes at the input end then the spot size can be continuously varied with a mode mixer that sharply bends the fiber and thereby shifts light to higher order modes. Spot size can also be varied by changing the taper length. Calculated irradiance profiles for a 400 μm core diameter fiber with a 0.22 numerical aperture and a divergence angle of 3.4° are shown in Fig. 3(b) for tapers ranging in length from 0.1 to 15 mm.

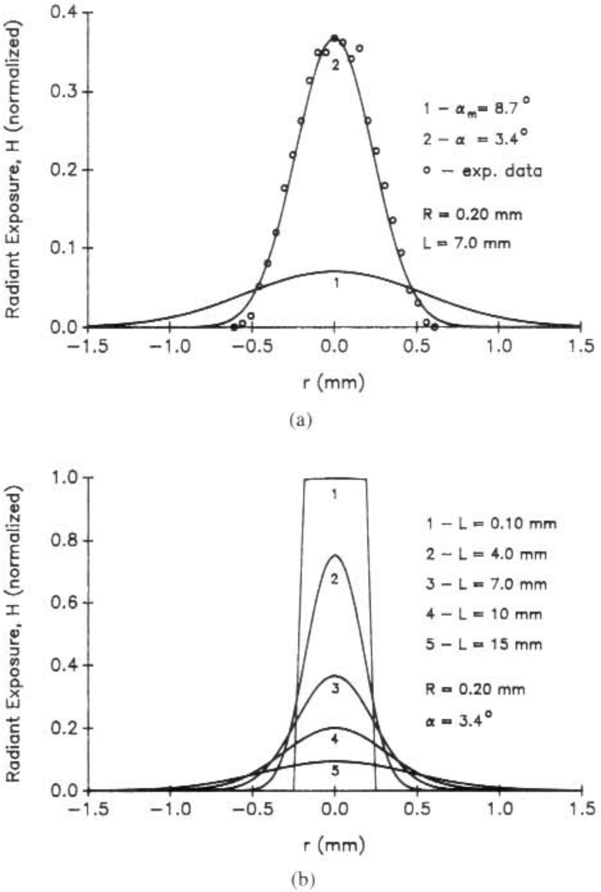

Fig. 3. (a) Curve 1 shows the calculated radiant exposure profile for the maximum beam divergence $a_{\text{maximum}} = 8.4°$ and curve 2 is for the actual beam divergence of 3.4°, which represents a considerably smaller spot size. The measured radiant exposure profile (circles) agrees well with the calculation. (b) Calculated radiant exposures for a 400 μm core diameter fiber with a beam divergence $a = 3.4°$, and various taper lengths demonstrating the effect of taper length on radiant exposure profile.

Testing in Human Arteries

Radiation at 480 nm was obtained from a flashlamp excited dye laser (Candela Laser Corp., Wayland, MA) using Coumarin 480 laser dye (Exciton Chemical Co., Dayton, OH) at a concentration of 1.5×10^{-4} molar in a 50 : 50 mixture of methanol and water. The typical 1–2 μs pulse duration was stretched to 8 μs by increasing the capacitance (5 μF) and inductance (16.5 μH) of the flashlamp driving circuit. This modified dye laser then produced 1 J pulses at a repetition rate of 10 Hz at the appropriate wavelength and pulse duration for maximizing selective ablation of plaque [23].

Because of thermal lensing, turbulence in the flowing laser dye and optical constraints, the laser did not have optimal mode quality. As a result, focusing the beam to a small spot on the fiber input end would create ''hot'' spots that could damage the input surface of the fiber. In order to minimize fiber damage, the laser beam was deliberately focused to a large waist that spread the beam over the entire fiber surface. In this way, radiation was coupled into quartz optical fibers with about 50–60% coupling efficiency using a 50 mm focal length quartz lens. The use of a relatively long focal length also resulted in excitation of only lower order fiber modes, resulting in a low divergence angle α, and hence, a relatively small spot size ($1/e^2$) of 0.95 mm for a 7 mm taper length (see Fig. 3(a) curve 2). This did, however, minimize the problem of optical breakdown at the fiber input end. Fortunately, when the fiber did fail, it was always due to optical breakdown at the input end and never at the output end near the ball tip. Laser and fiber output were periodically monitored using a power meter (Coherent Model 210, Palo Alto, CA) with the laser running at 3 Hz.

Human limbs were obtained fresh and studied within 6 h of amputation. Proximal ends of the arteries were identified, surgically exposed, and cannulated with a catheter. Arteriograms were performed by injecting a radiographic contrast solution through the catheter. This not only defined the arterial anatomy but also displaced all residual blood so that ablation would occur in a transparent field. In an artery that was not obstructed with plaque, the device could be advanced easily without dissection or perforation (Fig. 4) as long as the artery diameter was larger than the device. Using a curved catheter it was sometimes possible to deflect the tip enough to direct the device down a specific artery branch. Under fluoroscopy the stainless steel sleeve could be clearly seen with a distal faint radiolucency corresponding to the tapered ball tip. Contrast solution could be injected through a coaxial catheter to identify the position of the device within the arterial lumen.

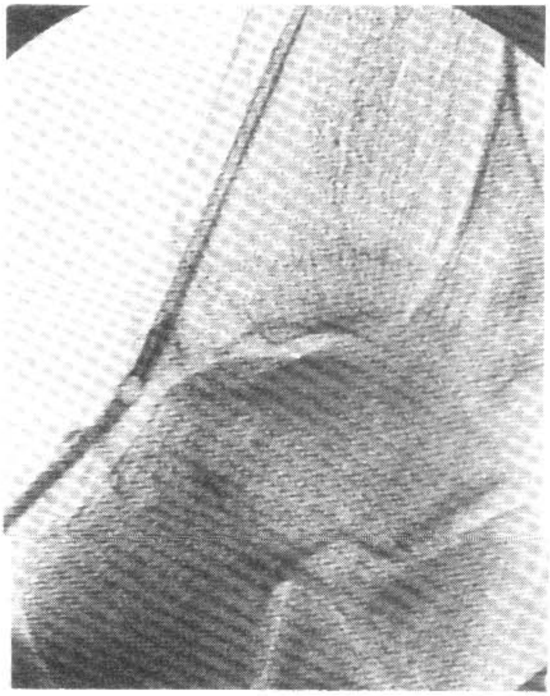

Fig. 4. A ball-tip fiber is shown inside the distal anterior tibial artery at the level of the ankle. The ball tip is seen as a lucency within a contrast filled artery.

In the first occluded artery, a 400 μm core fiber with a 2.5 mm ball tip and spot size ($1/e^2$) of 0.95 mm was inserted directly into the artery and advanced up to the point of obstruction under fluoroscopic guidance. The laser was activated at 3 Hz with a low-energy per pulse and the energy per pulse slowly increased until ablation could be heard and felt as a recoil force at the proximal end of the fiber. Ablation was first detected at 200 mJ/pulse (56 J/cm^2 based on a $1/e$ spot size of 0.67 mm) although minimal progress toward recanalization occurred at that energy. With the energy per pulse increased to 300 mJ (85 J/cm^2) and with the laser at 3 Hz, the fiber could be gently advanced with constant pressure through the obstruction. Periodically the fiber was removed to inject contrast solution for assessing the progress of recanalization. After irradiation, a final arteriogram was performed (Fig. 5). When the fiber abutted the arterial wall perpendicularly at a 90° bend in the artery, it was possible to ablate normal artery and perforate by increasing the energy to 800 mJ/pulse (226 J/cm^2).

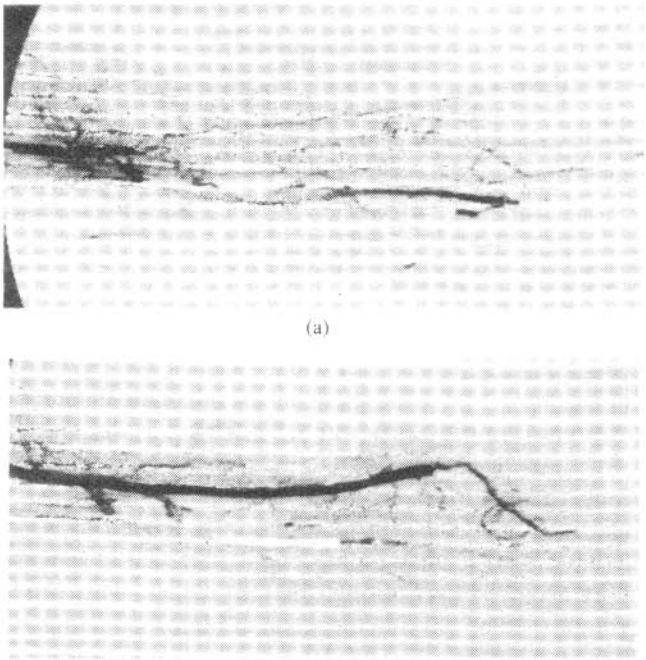

(a)

(b)

Fig. 5. A digital subtraction image of an occluded peroneal artery before irradiation (a) and after recanalization (b) with 480 nm radiation in 8 μs pulses delivered via a 400 μm core fiber with a 2.5 mm ball tip and a spot size ($1/e^2$) of 0.95 mm.

The typical rate of recanalization through plaque was about 100 pulses/cm although it varied enormously with plaque type. This was unreasonably slow at a 3 Hz repetition rate but when the laser was upgraded to operate at 10 Hz, it was about 10 s/cm and seemed adequate. Dissection or perforation occurred when the device was advanced too rapidly or into arteries that were smaller than the device. The recanalized channels were typically 2–3 mm in diameter, which is much larger than the spot size (see Figs. 5 and 6).

Damage to the fiber–optic delivery system was generally minimal. After several thousand ablative laser pulses, traces of 1 μm pitting on the ball surface were found. The fibers broke when deliberately bent to a radius of curvature of less than 5 mm for a 400 μm core diameter fiber, but the fractured ends were held together by the tough teflon jacket.

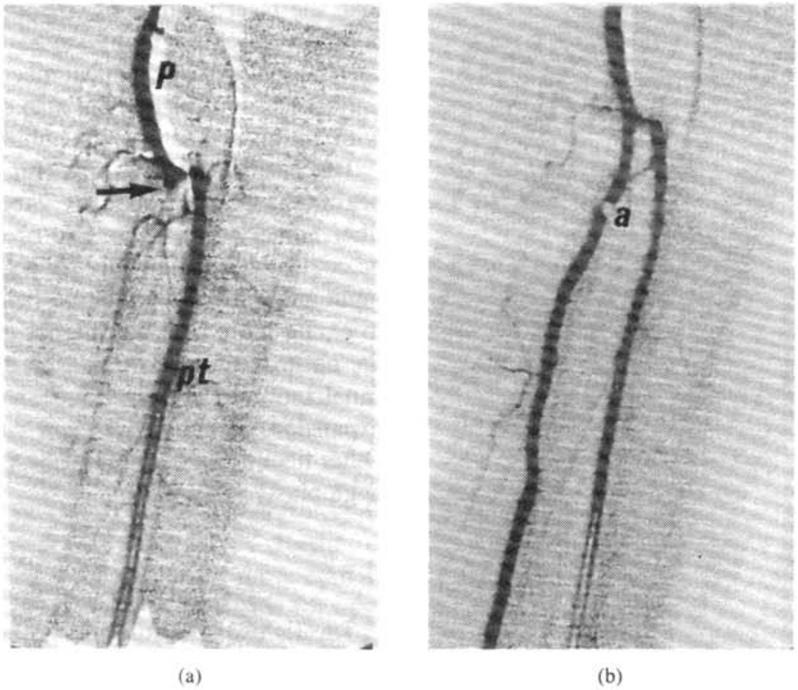

Fig. 6. Digital subtraction angiograms demonstrating recanalization of an occluded peroneal artery. Before laser irradiation (a) there are patent popliteal (P) and posterior tibial (pt) arteries but the peroneal artery is occluded (arrow) at the takeoff of the post tibial artery. The ball-tipped fiber was introduced into the popliteal artery, and advanced up to the site of occlusion (arrow) which was then irradiated with 800 pulses of 480 nm laser radiation at 8 us pulse duration and 260 mJ/pulse. After irradiation (b) the peroneal artery is widely patent and branches off the peroneal artery are well perfused indicating that the native lumen was recanalized. (Note also a small air bubble (a) in the proximal peroneal artery.)

Time-Delayed Flash Photography

The ability to create 2–3 mm channels with a laser spot size of less than 1 mm suggested an ablation mechanism that was more complicated than simple tissue ablation. To examine the mechanism of pulsed dye laser ablation of tissue with the ball-tipped fiber, time-delayed flash photography of ablation in yellow agar was performed. Transparent agar (Knox gelatin, 12% concentration in water by weight) was doped with sufficient yellow food coloring to confer an absorption coefficient of 50 cm^{-1} at 480 nm (to simulate plaque absorption at 480 nm). A hole in the side of an agar filled dish permitted introduction of the ball-tipped fibers into the agar without disturbing the agar surface. Ablation was performed with 1 μs pulses of 480 nm radiation from the pulsed dye laser. Another pulsed dye laser tuned to 633 nm was used to provide a 1 μs transilluminating flash pulse for a 35 mm camera that was oriented perpendicular to the ablating laser beam. A HeNe band-pass filter (633 nm) excluded the 480 nm laser radiation from exposing the film. The room was darkened sufficiently so that when the shutter was held open, the film (Kodak Plus-X) was exposed only by the 633 nm transilluminating flash. A delay circuit permitted triggering the illumination pulse to occur 1 to 800 μs after the ablative pulse. Photographs were taken of ablation by a 2.5 mm diameter ball-tip fiber with a 7 mm long taper at a radiant exposure found to recanalize occluded human peripheral arteries.

The photographs shown in Fig. 7 reveal that initially, vaporization of agar occurs in a region of the ball-tip surface corresponding to the region of irradiation. The irradiated agar forms an expanding vapor bubble that grows for several hundred μs after the arrival of the 1 μs ablative pulse to a size of the order of 5–6 mm in diameter. Then the vapor bubble collapses over a similar period of time.

Discussion

Safe delivery of laser radiation to obstructing plaques within arteries has been a major challenge of laser angioplasty. This study demonstrates a simple but effective method of introducing laser radiation into arteries with minimal mechanical injury. It utilizes a small diameter, flexible fiber that allows for recanalization of 2–3 mm diameter channels. There are no losses along the fiber from extra optical interfaces and the "stiff" region at the fiber tip is short. It readily transmits 480 nm radiation at sufficient irradiance to ablate calcified plaque with laser-induced plasma [10] and to selectively ablate yellow plaque [11], [12].

These tests of this fiber-optic device in human legs demonstrate its ability to effectively ablate calcified and soft plaque without perforating normal artery. The abla-

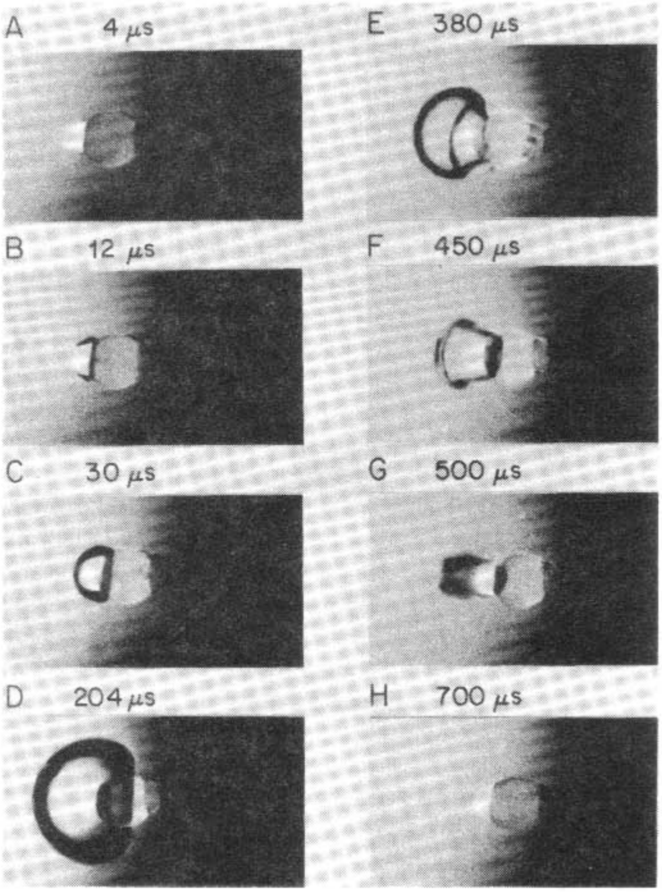

Fig. 7. Time-delayed photography. A ball-tipped fiber is submerged in a pool of yellow agar with an absorption coefficient comparable to human atherosclerotic plaque. A μs pulse of 480 nm radiation is fired down the fiber. With a radiant exposure just above ablation threshold, it vaporizes the agar (A). The vaporizing agar forms a high pressure steam bubble that expands to reach a maximum diameter of about 5 mm at about 200 μs after arrival of the laser pulse (D). This bubble then collapses over several hundred μs and is gone by 700 μs. This suggests a mechanism for laser angioplasty that involves not only ablation of tissue but also expansion of the artery lumen by a high-pressure bubble.

tion thresholds obtained here are higher than those obtained at shorter pulse durations and with a perpendicular angle of incidence but are in agreement with previously reported *in vitro* ablation threshold values with a similar device [24]. These values are also comparable to those reported for recanalizing peripheral arteries with pulsed 480 nm radiation in patients, given the differences in spot size [12].

The design appears to be "fail-safe." When laser intensity is too high the input end is destroyed before the intensity gets high enough to damage the output end, thus preventing an undesirable fiber failure inside a patient. If the fiber breaks it is held together by the tough teflon coating and does not break off. The ablative pulses do appear to slightly erode the tip of the fiber but the cumulative damage of several thousand pulses is negligible.

The ability to ablate large channels in the arteries below the knee is particularly exciting because it means that the laser procedure would not need to be augmented by balloon angioplasty as is the case with most laser systems at present. The ability to recanalize a channel much larger than the laser beam spot size was unexpected. Time-delayed, flash photography suggests an interaction of optical, thermal and mechanical mechanisms that involves not only ablation of plaque but also stretching open the artery with a high-pressure vapor bubble.

The laser beam spot size (for a highly divergent laser beam) can be controlled by varying fiber core diameter, fiber numerical aperture and/or taper length. It can also be controlled dynamically for a given fiber by varying the input angle of laser radiation being coupled into the fiber to excite more or fewer higher order modes. At present, the optimal spot size (i.e., the optimal ratio between recanalization by ablation to recanalization by vapor bubble expansion) is not known and deserves further research. Other fiber designs may also be suitable for selective laser angioplasty [24]–[28].

Appendix
Calculation of Fiber Spot Size

The light distribution at the ball tip depends upon the fiber diameter ($2R$), the taper length (L), the mode structure within the cylindrical part of the fiber and the diverging propagation with the tapered part of the fiber tip. At the transition between the cylindrical part of the fiber and the taper ($z = 0$, where z is coordinate along the optical axis), the energy E_0 is uniformly distributed across the fiber cross section according to the source function $S(\boldsymbol{r})$ where (bold signifies vector notation)

$$S(\boldsymbol{r}) = \begin{cases} \dfrac{E_0}{\pi R^2} & \text{for } 0 \le |\boldsymbol{r}| \le R \text{ and } z = 0 \\ 0 & \text{elsewhere} \end{cases} \tag{1}$$

If the angle of the taper is less than the angle of divergence α then the taper functions like an optical fiber and the distribution of optical energy will continue to be roughly uniform across the taper cross section. But, if α is sufficient to allow undisturbed beam expansion, then each point on the end of the cylindrical part of the fiber acts as a point source radiating light in an angular Gaussian distribution with divergence angle α. The light distribution due to all of the point sources within this cross section is given by [29]

$$H(\boldsymbol{r}) = \int G(\boldsymbol{r} - \boldsymbol{r}')\, S(\boldsymbol{r}')\, d\boldsymbol{r}' \tag{2}$$

where the Green's function $G(\boldsymbol{r})$ for a point source is

$$G(\boldsymbol{r}) = G(r, z) = \frac{z}{A(\alpha)\,(r^2 + z^2)^{1.5}}\, e^{(-2r^2/z^2 \tan^2 \alpha)} \tag{3}$$

and the normalization factor A is only dependent on the divergence angle α

$$A(\alpha) = 2\pi \left[1 - \frac{\sqrt{2\pi}}{\tan \alpha}\, e^{(2/\tan^2 \alpha)} \operatorname{erfc}\left(\frac{\sqrt{2}}{\tan \alpha} \right) \right] \tag{4}$$

Two special cases of (2) are of particular interest: the near field and the far field, which are solved by (5) and (6).

A. Near Field ($z \to 0$)

$$\lim_{z \to 0} H(\boldsymbol{r}) = S(\boldsymbol{r}). \tag{5}$$

B. Far Field ($z >> R$)

$$\lim_{R \to 0} H(\boldsymbol{r}) = \frac{E_0}{z^2} \frac{\cos^3 \theta}{A} e^{-2(\tan^2 \theta / \tan^2 \alpha)}$$

$$\text{where } \theta = \arctan\left(\frac{r}{z}\right). \tag{6}$$

Acknowledgment

The authors are particularly grateful for the guidance and continuing support of Dr. J. Parrish, Director of the Wellman Laboratory. They also thank Dr. N. Harris, the Pathology Department, and the operating room staff for assistance in obtaining specimens; B. Farinelli for assistance with time-delayed photography; J. DiBenedeto and R. Wheymouth for assistance with the X-ray imaging apparatus; S. Obremski for assistance with optical measurements, and Dr. R. Akhavan, Dr. R. Anderson, Dr. J. Frisoli, Dr. T. Sedlacek, Dr. A. Waltman, Dr. S. Geller, Dr. F. Steinberg, Dr. T. Deutsch, Dr. P. Ortu, and Dr. J. Roider as well as G. Finkenbeiner, L. Lilge, V. Venugopalau, and A. Seidlitz for many helpful discussions.

References

[1] R. Ginsberg, L. Wexler, R. S. Mitchell, and D. Profitt, "Percutaneous transluminal laser angioplasty for treatment of peripheral vascular disease, clinical experience with 16 patients," *Radiology*, vol. 156, pp. 619–624, 1985.

[2] G. Lee, R. M. Ikeda, J. H. Theis, M. C. Chan, D. Stobbe, C. Ogata, A. Kumagai, and D. T. Mason, "Acute and chronic complications of laser angioplasty: Vascular wall damage and formation or aneurysms in the atherosclerotic rabbit," *Amer. J. Cardiol.*, vol. 53, pp. 290–293, 1984.

[3] G. S. Abela, J. M. Seeger, E. Barbieri, D. Franzini, A. Fenech, C. J. Pepine, and C. R. Conti, "Laser angioplasty with angioscopic guidance in humans," *J. Amer. Coll. Cardiol.*, vol. 8, pp. 184–192, 1986.

[4] C. Borst, "Percutaneous recanalization of arteries: Status and prospects of laser angioplasty with modified fibre tips," *Lasers Med. Sci.*, vol. 2, pp. 137–151, 1987.

[5] R. R. Anderson and J. A. Parrish, "Selective photothermolysis: Precise microsurgery by selective absorption of pulsed radiation," *Science*, vol. 220, pp. 524–527, 1983.

[6] R. Birngruber, I. Hillenkamp, and V. P. Galeel, "Theoretical investigations of laser thermal retinal injury," *Health Phys.*, vol. 48, no. 6, pp. 781–796, 1985.

[7] L. I. Deckelbaum, J. M. Isner, R. F. Donaldson, S. M. Laliberte, R. H. Clarke, and D. M. Salem, "Use of pulsed energy delivery to minimize tissue injury resulting from carbon dioxide laser irradiation of cardiovascular tissues," *J. Amer. Col. Cardiol.*, vol. 7, pp. 898–908, 1986.

[8] W. S. Grundfest, I. F. Litvack, T. Goldenberg, T. Sherman, L. Morgenstern, R. Carroll, M. Fishbein, J. Forrester, J. Margitan, S. McDermid, T. J. Pacala, D. M. Rider, and J. B. Laudenslager, "Pulsed ultraviolet lasers and the potential for safe laser angioplasty," *Amer. J. Surg.*, vol. 150, pp. 220–226, 1985.

[9] M. R. Prince, G. M. LaMuraglia, P. Teng, T. F. Deutsch, and R. R. Anderson, "Selective ablation of calcified arterial plaque with laser-induced plasmas," *IEEE J. Quantum Electron.*, vol. QE-23, pp. 1783–1786, 1987.

[10] M. R. Prince, T. F. Deutsch, M. M. Mathews-Roth, R. Margolis, J. A. Parrish, and A. R. Oseroff, "Preferential absorption in atheromas in vitro: Implications for laser angioplasty," *J. Clinic. Investig.*, vol. 78, pp. 295–302, 1986.

[11] M. R. Prince, T. F. Deutsch, A. H. Shapiro, R. J. Margolis, A. R. Oseroff, J. T. Fallon, J. A. Parrish, and R. R. Anderson, "Selective laser ablation of atheromas using a flashlamp-excited dye laser at 465 nm," *Proc. Nat. Acad. Sci. USA*, vol. 83, pp. 7064–7068, 1986.

[12] A. Murray, R. F. M. Wood, D. C. Mitchell, D. H. Edwards, M. Grasty, and R. Basu, "Peripheral laser angioplasty with pulsed dye laser and ball-tipped optical fibers," *Lancet*, pp. 1471–1474, Dec. 23–30, 1989.

[13] H. J. Geschwind, J.-L. Dubois-Rande, E. Shafton, G. Boussigac, and M. Wexman, "Percutaneous pulsed laser assisted balloon angioplasty guided by spectroscopy," *Amer. Heart J.*, vol. 117, no. 5, pp. 1147–1152, 1989.

[14] D. L. Singleton, G. Paraskevopoulos, R. S. Taylor, and L. A. J. Higginson, "Excimer laser angioplasty: Tissue ablation, arterial response, and fiber optic delivery," *IEEE J. Quantum Electron.*, vol. QE-23, pp. 1772–1782, 1987.

[15] M. R. Prince, G. M. LaMuraglia, and E. F. MacNichol, "Increased preferential absorption in atherosclerotic plaque with oral beta carotene: Implications for laser endarterectomy," *Circulation*, vol. 78, pp. 338–344, 1988.

[16] M. L. Wolbarsht, "Laser surgery: CO_2 or HF," *IEEE J. Quantum Electron.*, vol. 20, pp. 1427–1432, 1984.

[17] J. M. Isner and R. H. Clarke, "Laser Angioplasty: Unraveling the gordian knot," *J. Amer. Coll. Cardiol.*, vol. 7, pp. 705–708, 1986.

[18] T. A. Sanborn, "Laser Angioplasty: What has been learned from experimental studies and clinical trials," *Circulation*, vol. 78, pp. 769–779, 1989.

[19] V. Russo, G. C. Righini, S. Sottini, and S. Trigari, "Lens-ended fibers for medical applications: A new fabrication method," *Appl. Opt.*, vol. 23, pp 327, 1984.

[20] E. Pilger, J. Lammer, R. Kleinert, J. Ascher, and H. Bertuch, "Laser angioplasty with a contact probe for the treatment of peripheral vascular disease," *Cardiovascular Res.*, vol. 22, pp. 149–153, 1988.

[21] R. M. Verdaasdonk, F. W. Cross, and C. Borst, "Physical properties of sapphire fibretips for laser angioplasty," *Lasers Med. Sci.*, vol. 2, pp. 183–188, 1987.

[22] R. U. Verdaasdonk, "Laser angioplasty with modified fiber tips," Ph.D. dissertation, Univ. Hospital, Utrecht, The Netherlands, 1990.

[23] G. M. LaMuraglia, S. Murray, R. R. Anderson, and M. R. Prince, "Effect of pulse duration on selective ablation of atherosclerotic plaque by 480–490 nm radiation," *Lasers Surg. Med.*, vol. 8, pp. 18–21, 1988.

[24] C. E. Seidlitz, "Development and testing of new transmission systems for peripheral laser angioplasty," M.S. thesis, Cologne Inst. Technol., Cologne, W. Germany, 1990.

[25] S. Sottini, V. Russo, G. Marghe, and F. Crea, "Probe for laser angioplasty radiating a corolla shaped beam," *Appl. Opt.*, vol. 28, pp. 995–999, 1989.

[26] R. M. Cothren, G. B. Hayes, J. R. Kramer, B. Sacks, C. Kittrell, and M. S. Feld, "A multifiber catheter with an optical shield for laser angiosurgery," *Lasers Life Sci.*, vol. 1, pp. 1–12, 1986.

[27] V. Russo, "Optical fibre delivery systems for laser angioplasty and laser treatment of tumours," *Lasers Med. Sci.*, vol. 3, pp. 207–211, 1987.

[28] A. Katzir, "Optical fibers for medicine," *Sci. Amer.*, vol. 260, pp. 120–126, 1985.

[29] S. A. Prahl, M. Keijzer, S. L. Jacque, and A. J. Welch, "A Monte Carlo model of light propagation in tissue," *Proc. SPIE*, 1988.

Martin R. Prince graduated from Harvard Medical School in 1985, interned in medicine at the University of California, San Francisco, and received the Ph.D. degree from Massachusetts Institute of Technology, Cambridge, in 1988 studying fundamental aspects of the interaction of high-intensity radiation with cardiovascular tissues.

He is now with the Wellman Laboratories of Photomedicine at Massachusetts General Hospital, Boston, and is a Clinical Fellow with the Department of Radiology at Harvard Medical School, continuing studies of light–tissue interactions.

Glenn M. LaMuraglia, for a photograph and biography, see this issue, p. 2206.

Christine E. Seidlitz received the M.S. degree in engineering from the Cologne Institute of Technology, Cologne, Germany, and recently completed her Ph.D. dissertation research on optical delivery systems for angioplasty laser at the Wellman Laboratories of Photomedicine, Harvard Medical School, Massachusetts General Hospital, Boston, MA.

Scott A. Prahl received the B.S. degree in applied physics from the California Institute of Technology, Pasadena, and the Ph.D. degree in biomedical engineering from the University of Texas, Austin, in 1982 and 1988, respectively.

He is currently performing postdoctoral research developing medical diagnostic techniques using light transport in tissue with the Wellman Laboratories of Photomedicine, Harvard Medical School, Massachusetts General Hospital, Boston, MA.

Christos A. Athanasoulis is associate director of Radiology at Massachusetts General Hospital and Professor of Radiology at Harvard Medical School. He has been a pioneer in the development of modern angiographic techniques for the past 20 years and is currently directing trials of percutaneous laser angioplasty in peripheral arteries at Massachusetts General Hospital, Boston.

Reginald Birngruber, for a photograph and biography, see this issue, p. 2147.